Dissolution Kinetics and Porosity Development in Carbonates under Seawater-Assisted HCl Acidizing

Amir Hossein Saeedi Dehaghani* , Hadi Tanhaei

Department of Petroleum Engineering, Faculty of Chemical Engineering, Tarbiat Modares University of Tehran, Iran

***: asaeedi@modares.ac.ir**

Abstract

Carbonate reservoirs account for nearly 50% of global proven oil reserves, with 70% in the Middle East occurring in fractured formations. Moreover, their heterogeneous pore structures and oil-wet surfaces limit recovery efficiency. Furthermore, matrix acidizing is a well-established stimulation technique to improve productivity in carbonate reservoirs; however, its success is strongly influenced by acid composition, ionic strength of the carrier fluid, and surface wettability conditions. This study experimentally evaluates the effects of acid concentration (15% and 28% HCl), brine composition (distilled water vs. seawater), and surfactant pre-flush (CTAB) on the dissolution kinetics and porosity evolution of carbonate cores under both oil-free and oil-saturated conditions. Also, laboratory experiments were conducted on core samples at 26 °C using controlled acid injection tests. Moreover, the initial contact angle

(~140°) confirmed the strongly oil-wet nature of the untreated rock surface. In addition, results revealed that seawater-based acid systems produced more stable wormholes, 20–35% higher porosity enhancement, and approximately 15% lower sludge formation compared with distilled-water-based acids. Also, the CTAB pre-flush significantly improved acid accessibility, reduced CO_2 bubble blockage, and enhanced dissolution uniformity, particularly under oil-saturated conditions. Ultimately, these findings demonstrate that combining seawater-based acids with surfactant-assisted pre-treatment provides a more sustainable, efficient, and field-applicable strategy for carbonate reservoir stimulation.

Keywords: Carbonate Reservoirs, Recovery Efficiency, Matrix Acidizing, Wormhole

Introduction

Carbonates account for more than half of the world's oil reserves and, due to their unique depositional settings, complex diagenetic histories, and highly heterogeneous pore systems, they play a strategic role in global energy supply [1]. These formations include limestones, dolomites, and chalks, which they exhibit strong mineralogical variability, high fracture density, and complex pore connectivity resulting from multistage diagenetic alterations such as recrystallization, dissolution, and cementation. In addition, the combination of these geological features makes fluid flow within carbonates extremely non-uniform, where the majority of production often occurs through a limited number of high-permeability streaks or fractures. About 50% of the world's proven oil reserves are located in the Middle East, nearly 70% of which are hosted in fractured carbonate formations. Recent investigations have explored various techniques to enhance oil recovery from reservoirs, including matrix acidizing and surfactant flooding **[1, 2].** Their enormous storage capacity and widespread occurrence make carbonate reservoirs crucial for sustaining global hydrocarbon production. However, these same characteristics also pose severe production challenges, particularly due to complex pore structures, high capillary pressure, and variations in wettability that hinder efficient oil displacement **[3].**

Physical and chemical processes such as mineral dissolution and precipitation, changes in surface wettability, and strong capillary forces significantly reduce the natural productivity of carbonate reservoirs **[3]**. These processes are often intensified during drilling, completion, and production operations, leading to near-wellbore damage, formation plugging, or partial pore blockage. Such damage severely limits the effective permeability and thereby reduces hydrocarbon inflow to the wellbore. Hence, advanced stimulation and restoration techniques are required to restore or enhance well productivity [4]. Among these techniques, matrix

acidizing has emerged as the predominant and most cost-effective approach for treating carbonate reservoirs **[5–8]**. The main purpose of matrix acidizing is to dissolve acid-soluble minerals (calcite, dolomite, chalk) within the rock matrix, thereby increasing pore throat size, reducing skin factor, and improving overall formation conductivity **[5, 9, 10]**.

A conventional acidizing operation consists of three main stages: pre-flush, main acid injection, and over-flush. Each stage plays a critical role in the overall stimulation outcome. The pre-flush stage, which commonly employs brines, diesel, or surfactant-based fluids such as **cetyltrimethylammonium bromide (CTAB)**, serves several functions: it (1) displaces the resident formation fluids, conditions the rock surface, (2) alters wettability, and (3) minimizes the risk of sludge or emulsion formation during acid contact **[6, 11]**. In addition, proper pre-flush design also removes scale or iron precipitates and improves acid contact efficiency in the main stage.

The main acidizing stage involves injecting hydrochloric acid (HCl) at concentrations typically ranging from 5 wt.% to 28 wt.%, with 15 wt.% being the most widely used formulation in field applications [6, 12, 13]. The injected acid reacts with carbonate minerals, producing carbon dioxide and soluble calcium or magnesium chlorides. Moreover, this reaction creates conductive channels or wormholes that significantly enhance the permeability of the near-wellbore zone. In addition, the efficiency of wormhole propagation and the final stimulation performance depend strongly on multiple parameters such as temperature, acid concentration, injection rate, mineral composition, and fluid transport properties **[13]**. If the reaction rate is too high, the acid may be consumed near the wellbore, resulting in localized face dissolution and poor penetration. Conversely, if the reaction is too slow, the acid can bypass reactive zones without effectively dissolving the rock, reducing stimulation effectiveness. Achieving an

optimum balance between reaction kinetics and mass transfer is thus essential for successful acidizing design.

Wettability plays a decisive role in determining acid–rock interaction efficiency, especially in oil-wet carbonate formations **[11, 15]**. In such systems, the rock surface is coated with a thin film of adsorbed polar organic molecules (asphaltenes, resins, or fatty acids), which inhibits direct acid–rock contact and reduces dissolution efficiency. Therefore, wettability alteration during the pre-flush stage is a critical prerequisite for improving acid accessibility and ensuring uniform dissolution. Moreover, surfactant-based pre-flush fluids such as CTAB can modify the surface charge, desorb organic films, and convert the rock toward a more water-wet state, thereby facilitating deeper acid penetration into the matrix.

Additionally, the reduction of interfacial tension (IFT) between the injected acid and the reservoir fluids plays a vital role in enhancing displacement efficiency. Lowering IFT improves the ability of the acid to penetrate fine pore throats, displace trapped hydrocarbons, and prevent phase trapping during acid–rock reaction **[11, 16]**. This effect becomes even more critical in mixed-wet and oil-wet carbonate formations, where capillary forces oppose acid entry into smaller pores. Therefore, surfactants and ionic modifiers can substantially enhance both acid penetration and subsequent fluid flow, leading to higher permeability restoration and improved well productivity.

Also, recent advancements have focused on coupling chemical additives, optimized injection rates, and multi-stage stimulation designs to further improve acid distribution and control reaction fronts. These improvements have made matrix acidizing not only a remediation technique but also a strategic production enhancement tool in modern carbonate reservoir management. In addition, continuous integration of chemical, petrophysical, and reservoir

engineering approaches continues to evolve this technology toward more environmentally friendly, efficient, and cost-effective practices.

Carbonate reservoirs constitute more than 60% of the world's oil and gas reserves and are often characterized by (1) high heterogeneity, (2) low matrix permeability, and (3) intricate pore–fracture systems. Moreover, their production performance is highly dependent on effective stimulation techniques capable of restoring or enhancing fluid connectivity between the formation and the wellbore. Among these techniques, matrix acidizing remains one of the most widely applied and economically viable methods for carbonate formations, primarily aiming to dissolve formation damage, remove scale and mud filtrates, and enlarge existing pore throats through controlled acid–rock reactions. By injecting reactive acid solutions into the formation, the near-wellbore permeability can be significantly improved, facilitating hydrocarbon flow toward the production well **[17]**. However, the overall efficiency of the acidizing process depends on a delicate interplay between the acid reaction rate, mass transport mechanisms, reservoir temperature, and rock mineralogy, all of which jointly determine the pattern of dissolution and the development of conductive flow channels.

The fundamental mechanisms of acid–rock interaction have been extensively investigated over the past several decades. Fredd and Fogler **[18]** were among the first to systematically classify dissolution regimes in carbonate matrices, identifying the transitions between face dissolution, conical or wormhole formation, and uniform dissolution. In addition, their seminal work revealed that the optimal stimulation regime exists when acid reacts at a rate that allows deep penetration before being fully consumed—resulting in the development of dominant wormholes that connect the wellbore to undamaged zones. Subsequent experimental and numerical efforts by Ghommem et al. [19], Liu et al. [20], and Al-Arji et al. [21] further refined these models by coupling fluid flow dynamics, diffusion processes, and reaction kinetics. These studies highlighted the influence of temperature, acid diffusivity, and rock heterogeneity on

wormhole geometry and breakthrough efficiency, providing a quantitative framework for predicting acid penetration depth and optimum injection rate.

Despite significant advances in understanding transport–reaction coupling, the chemical composition of the acid system remains one of the most critical determinants of stimulation success. Furthermore, conventional hydrochloric acid (HCl) reacts vigorously with carbonate minerals such as calcite and dolomite, but its rapid reaction near the wellbore leads to premature acid spending, surface face dissolution, and limited penetration depth. Moreover, to overcome this limitation, researchers have developed retarded or controlled-reaction acid systems, including emulsified acids, gelled acids, and organic–inorganic acid blends such as HCl–acetic acid or HCl–formic acid mixtures **[22]**. These systems regulate the acid–rock contact and slow down the reaction rate by forming diffusion barriers or viscosity-controlled interfaces; thereby, allowing the acid to penetrate deeper before exhaustion. Numerous field and laboratory studies have confirmed that such hybrid systems effectively balance reactivity and diffusion, minimizing corrosion and sludge formation while producing more stable wormhole networks **[23].**

Beyond acid chemistry, brine composition and formation water chemistry have emerged as equally critical factors governing acidizing efficiency. The ionic structure of the injected fluid can significantly influence mineral dissolution pathways, surface charge distribution, and precipitation dynamics. In recent years, the concept of smart water or ionically engineered brines has gained attention in carbonate stimulation and enhanced oil recovery applications. The researches on low-salinity and seawater-based systems has demonstrated that the presence of specific ions, notably SO_4^{2-}, Mg^{2+}, and Ca^{2+}, can promote the desorption of adsorbed carboxylic species and shift the rock's wettability toward a more water-wet state [24,25]. This wettability alteration improves the contact efficiency between the acid and the rock surface, enhances dissolution uniformity, and facilitates the removal of trapped hydrocarbons.

Moreover, ion-tuned brines can suppress unwanted secondary precipitates such as $CaSO_4$, $Fe(OH)_3$, and CaF_2, while stabilizing fine particles during acid–rock reactions—thus improving long-term permeability retention [26].

The integration of engineered brines with acid systems has therefore become an important research frontier. Studies by Buriro et al. [27] and Nande et al. [28] revealed that careful adjustment of ionic composition, especially the ratio of divalent to monovalent ions, can significantly alter surface charge distribution, reaction front morphology, and wormhole structure. For instance, the presence of Mg^{2+} and SO_4^{2-} ions in seawater was found to reduce excessive local reactivity, resulting in smoother dissolution profiles and reduced acid–rock incompatibility. Consequently, seawater-based acids provide a more environmentally sustainable, cost-effective, and thermally stable alternative to conventional HCl systems, particularly for offshore carbonate reservoirs where seawater is readily available.

Another critical aspect of carbonate acidizing is acid–oil compatibility, especially in formations containing heavy or asphaltenic crudes. Moreover, strong acids can react with certain crude oil components—such as asphaltenes, naphthenic acids, and resin fractions—to form viscous, tar-like sludge. In addition, this sludge deposition blocks pore throats and significantly reduces permeability, offsetting the benefits of stimulation [29]. Furthermore, to mitigate this problem, chemical additives such as anti-sludge agents and surfactants have been widely applied. In addition, among these, cationic surfactants like cetyltrimethylammonium bromide (CTAB) have demonstrated excellent performance in stabilizing acid–oil emulsions, reducing interfacial tension (IFT), and preventing asphaltene aggregation during acidizing [30]. Furthermore, surfactant-assisted acid systems can alter rock wettability from oil-wet to water-wet, enhancing both acid penetration and post-treatment fluid flow. Studies by Jafari and Madadizadeh **[31]** have further shown that CTAB pre-flush treatments not only suppress sludge

formation but also facilitate the uniform distribution of acid across the pore network, leading to improved dissolution efficiency and higher permeability restoration.

Taken together, these findings suggest that modern carbonate acidizing is evolving toward multi-component, chemically balanced systems that combine acid strength control, ionic regulation, and interfacial modification. Such integrated approaches are essential for achieving deep, uniform dissolution, reduced environmental impact, and sustainable stimulation performance under diverse reservoir conditions.

The key difference between carbonate and sandstone acidizing lies in the reaction mechanism, sandstone acidizing mainly reopens blocked pores, whereas carbonate acidizing both removes damage and dissolves the rock matrix itself. Moreover, challenges such as salt precipitation and asphaltene sludge require careful process design Jafari and Madadizadeh in 2025 demonstrated that spent acid, with lower pH and higher viscosity than fresh acid, exhibits higher dissolution rates and diffusion coefficients for dolomite, partly due to unusual ion effects from impurities like iron and aluminum oxides **[31].**

The synergistic integration of acid, smart brine, and surfactant is now being recognized as the next frontier in carbonate stimulation design. While each component—acid type, brine salinity, and surfactant chemistry—has been individually explored, few studies have systematically examined their combined influence under real crude-oil conditions. Most published work relies on synthetic cores or simplified fluid systems that fail to capture the complex interactions among acid reactivity, ionic effects, and surface wettability changes. Therefore, the present study aims to fill this research gap by conducting a comprehensive experimental evaluation of carbonate core samples exposed to various acid formulations (HCl and HCl–acetic acid), brine types (deionized water and seawater), and CTAB surfactant concentrations. Specifically, the study examines how these parameters influence core mass loss, porosity change, and surface

morphology, supported by statistical analysis of dissolution trends. The results provide new insights into optimizing acidizing fluids to achieve deeper penetration, minimize sludge formation, and enhance recovery efficiency in carbonate reservoirs. Furthermore, the findings contribute to developing integrated acid–brine–surfactant stimulation strategies tailored to reservoir-specific conditions, bridging the gap between laboratory-scale experiments and field-scale implementation.

In this study, initially, contact angle tests are performed on thin sections saturated with oil. These samples are then exposed to various concentrations of surfactant solutions over different periods of time. Subsequently, the contact angle test is repeated to determine the extent of wettability alteration for each sample. This allows us to identify the optimal surfactant concentration and the ideal contact time between the surfactant and the rock for use in an acidic solution. Next, porosity tests are conducted on core samples. The prepared cores are then exposed to different acidic solutions. The weight of each core is measured before and after the test and the results are compared. Finally, the porosity test is repeated, and the results are presented.

This research explores the impact of pre-flush fluid on the acidizing process of carbonate cores. In this study, **cetyl trimethyl ammonium bromide (CTAB),** a cationic surfactant, is employed as the pre-flush fluid. Additionally, hydrochloric acid at a concentration of 15 and 28 wt.% is used to perform the acidizing treatment on the carbonate core.

Materials and Methods

Rock Sample

In this research, a representative carbonate rock specimen was selected to evaluate the influence of microwave exposure on surface wettability during the acidizing process. The chemical composition of the rock was determined using X-ray fluorescence (XRF), and the results are summarized in **Table 1**. According to this analysis, calcium carbonate ($CaCO_3$) constitutes approximately 95.9 wt.% of the total composition, indicating a high-purity carbonate matrix. In addition, to further confirm the mineralogical framework, X-ray diffraction (XRD) analysis was performed on powdered and thin-section samples of the same rock. The diffraction patterns revealed that the dominant crystalline phase is calcite ($CaCO_3$), with minor amounts of gypsum, microcline, muscovite, and trace dolomite and clay minerals. These findings confirm that the rock exhibits a clean, homogeneous carbonate texture consistent with typical reservoir formations.

Carbonate core plugs with dimensions of 3.8 cm in diameter and 5 cm in length were prepared from representative outcrop blocks of the Asmari Formation, one of the principal carbonate reservoirs in southwest Iran. Moreover, the mineralogical and geochemical characterization verified that these samples are suitable for controlled acidizing and wettability experiments. Furthermore, the crude oil used throughout the wettability, viscosity, and interfacial tension measurements was obtained from the same oil field and stratigraphic unit as the rock samples, ensuring geochemical compatibility between the rock and the fluid system. Also, the oil is classified as a moderately light asphaltenic crude with an API gravity of approximately 30°, an acid number of 0.76 mg KOH/g, and an asphaltene content of 16.8 wt.%. Furthermore, these

values are consistent with those typically found in the Asmari Formation and minimize experimental bias by replicating realistic reservoir conditions for acid–rock–oil interaction studies.

It should be noted that the specimens originated from the same geological source as those investigated by Tanhaei et al. in 2023, confirming the consistency and representativeness of the selected materials. The XRD spectrum obtained from the powdered samples is presented in **Figure 1**, which clearly displays the characteristic diffraction peaks of calcium carbonate along with minor contributions from accessory minerals **[12]**.

Table 1. XRF of Carbonate Rock.

Mineral	Measured, oxide-basis (wt.%)	Converted, carbonate-equivalent (wt.%)	Normalized on converted basis (wt.%)
Na_2O	0.035	0.035	0.033814
$MgCO_3$	0.565	1.181938	1.141874
Al_2O_3	0.178	0.178	0.171966
SiO_2	0.697	0.697	0.673374
P_2O_5	0.081	0.081	0.078254
SO_3	0.735	0.735	0.710086
Cl	0.009	0.009	0.008695
K_2O	0.037	0.037	0.035746
$CaCO_3$	55.675	99.36717	95.99893
TiO_2	0.067	0.067	0.064729
Fe_2O_3	0.146	0.146	0.141051
$SrCO_3$	0.684	0.974512	0.941479

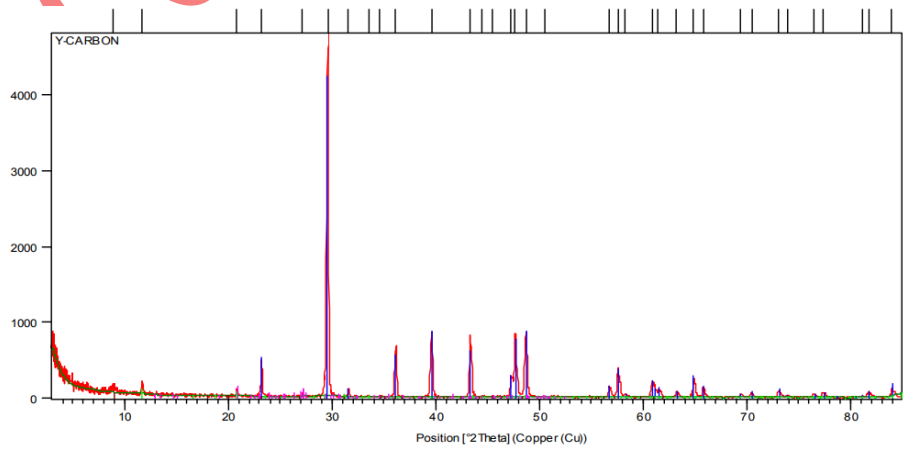

Fig 1. The XRD spectrum of the pulverized carbonate rock section. (Also, used by Tanhaei et al. 2023 **[12]**)

Oil Sample

The oil sample was sourced from a southern oil field in Iran. **Table 2** displays the crude oil properties. In addition, the composition of oil sample employed to conduct the tests is shown in **Table 3**. The asphaltene content of crude oil samples was determined using the IP-143 standard method. Moreover, oil was mixed with n-heptane, refluxed, and left for 24 h to allow precipitation, followed by filtration to separate asphaltene and wax. Furthermore, the waxes were washed out with heptane, the asphaltenes were dissolved in toluene, and after solvent evaporation, the remaining asphaltene fraction was weighed to calculate its percentage. In addition, viscosity measurements were performed using an Anton Paar rheometer equipped with a CC27 spindle, capable of operating up to 1200 rpm and shear rates of 1400 s^{-1}. In addition, the device measures viscosity by recording the resistance exerted on the rotating spindle within the fluid chamber, with sensors capturing force and temperature data. In this study, 18 cc of crude oil was tested under varying temperatures to evaluate the effects of acid treatment and microwave exposure on viscosity. Also, the density of crude oil samples was determined using a 10 cc pycnometer, where the liquid mass was obtained from the weight difference of the filled and empty vessel. Moreover, the density was then calculated as the ratio of mass to volume. All measurements were carried out at a controlled temperature of 26 °C to minimize error. Interfacial tension (IFT) between oil and water strongly influences capillary forces and, consequently, oil recovery efficiency. Moreover, chemical agents such as surfactants, alkalis, and polymers reduce IFT, enhancing residual oil mobilization. In

this study, IFT was accurately measured using the hanging drop method, where drop images are analyzed via the Young–Laplace equation **[13,14].**

Table 2. Crude oil properties at 26 °C **[13]**.

Asphaltene (%)	Viscosity (cP)	Density (gr/cc)	IFT
16.83	537	0.943	**35.69**

Table 3. The composition of oil sample used for aging the rock sections **[14]**.

Components	Mole weight	Flashed Liquid
Nitrogen	28.01	0
Carbon Dioxide	44.01	0
Hydrogen Sulfide	34.08	0.0004
Methane	16.04	0
Ethane	30.07	0
Propane	44.1	0.139
I – Butane	58.1	0.127
N – Butane	58.12	1.318
I – Pentane	72.15	1.107
N – Pentane	72.15	3.105
Pseudo C_6H_{14}	84	6.109

Pseudo C_7H_{16}	96	9.316
Pseudo C_8H_{18}	107	9.478
Pseudo C_9H_{20}	121	8.252
Pseudo $C_{10}H_{22}$	134	7.054
Pseudo $C_{11}H_{24}$	147	6.568
Pseudo $C_{12}H_{26}$	161	5.547
Pseudo $C_{13}H_{28}$	175	4.16
Pseudo $C_{14}H_{30}$	190	3.813
Pseudo $C_{15}H_{32}$	206	3.12
Pseudo $C_{16}H_{34}$	222	2.427
Pseudo $C_{17}H_{36}$	237	2.08
Pseudo $C_{18}H_{38}$	251	1.733
Pseudo $C_{19}H_{40}$	263	1.387
Pseudo $C_{20}H_{42}$	277	1.248
Pseudo $C_{21}H_{44}$	291	1.04
Pseudo $C_{22}H_{46}$	305	0.832
Pseudo $C_{23}H_{48}$	318	0.763
Pseudo $C_{24}H_{50}$	331	0.693
Pseudo $C_{25}H_{52}$	345	0.555
Pseudo $C_{26}H_{54}$	359	0.485
Pseudo $C_{27}H_{56}$	374	0.416
Pseudo $C_{28}H_{58}$	388	0.347
Pseudo $C_{29}H_{60}$	402	0.277
C30+	935	16.666
Total	**-**	**100**

Surfactant (CTAB)

In this study, the cationic surfactant **Cetyltrimethylammonium Bromide (CTAB)** was employed to investigate its effect on rock surface wettability and subsequent acidizing performance. Initially, carbonate thin sections were exposed to various CTAB concentrations (250, 370, and 500 ppm) at 70 °C for controlled contact times of 60 and 120 minutes. The wettability alteration was then evaluated through contact angle measurements to determine the optimum surfactant dosage and exposure duration for use in subsequent acidizing experiments. For solution preparation, CTAB was dissolved in both deionized water and seawater using a magnetic stirrer to ensure homogeneity. A schematic representation of the CTAB molecular structure is illustrated in **Fig. 2 [13]**.

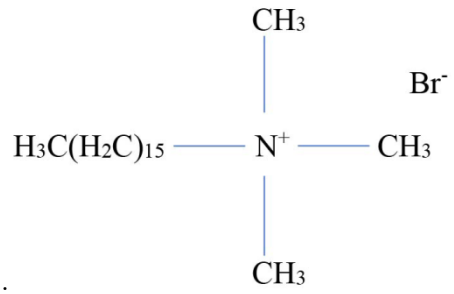

Fig. 2 A schematic of CTAB [17].

The initial contact angle of the untreated carbonate surface was approximately 140°, confirming the strongly oil-wet nature of the rock prior to surfactant exposure. Detailed contact angle tests were conducted only for surface verification and are not presented herein.

Acid Solution

The acid solutions were prepared at a concentration of 15% and 28% to mimic the rock-acid interaction at the beginning of injection. Two base water of distilled water and seawater were used to synthesize the acid solutions. The composition of seawater, which is shown in **Table 4**, was adopted from the Persian Gulf seawater. The HCl concentrations of 15 wt.% and 28 wt.% were selected to represent typical field acidizing formulations and the upper laboratory limit for comparative dissolution studies, respectively.

Table 4. The composition of brine water compositions (sea water and distilled water) **[15]**.

Composition	Concentration(ppm)	
	Distilled water	Seawater
NaCl	0	28323
Na_2SO_4	0	4936
$CaCl_2$	0	1630
$MgCl_2.6H_2O$	0	10510
KCl	0	1032
TDS	0	46431

Sample Preparation

The sea water of the Persian Gulf was used in this research. Also, 30.2% HCl was used to prepare acidic solutions, which were diluted to 15% and 28 % wt. using distilled water and sea water **[15].**

The acidic solutions used are acidic sea water and acidic distilled water, acidic water is the water used to dilute the mother hydrochloric acid (30.2%). In this study, highly porous carbonate core samples were selected, and their porosity was determined using a helium porosimeter. Moreover, each measurement was conducted in triplicate to ensure reliability, and the obtained results (presented in **Table 5**) showed a measurement error of less than 1%. It should be noted that cores **4, 6, 13, and 14** have already been discussed in the references **[13,15]**.

Table 5. Porosity test results of cores [13].

Core No.	Diameter (cm)	Height (cm)	Pore Volume (cc)	Porosity (%)
1	3.81	0.85	5.034	51.941
2	3.81	0.8	4.511	49.462
3	3.81	0.9	4.677	45.583
4	3.81	0.9	4.416	43.04

5	3.81	0.9	4.857	47.338
6	3.81	0.9	4.466	43.529
7	3.81	0.8	4.148	45.482
8	3.81	0.85	4.184	43.171
9	3.81	0.8	3.878	42.523
10	3.81	0.85	4.131	42.631
11	3.81	0.85	4.714	48.64
12	3.81	0.7	3.714	46.542
13	3.81	0.85	4.367	45.067
14	3.81	0.8	4.197	46.019
15	3.81	0.75	3.781	44.213
16	3.81	0.9	4.303	41.935
17	3.81	0.75	3.736	43.695
19	3.81	0.9	4.827	47.047
20	3.81	0.8	4.172	45.746
21	3.81	0.9	5.002	48.751

Porosimeter

Porosity is regarded as one of the key petrophysical properties of reservoir rocks, as it directly reflects their ability to store and transmit fluids. An accurate determination of this parameter is essential for evaluating hydrocarbon reserves and predicting production performance. In the present work, the porosity of carbonate core plugs was carefully measured both prior to and following the acidizing treatment, allowing the influence of the stimulation process on the pore system to be assessed. Also, the measurements were carried out using a helium porosimeter, which provides reliable results by injecting helium gas into the sample and recording the pressure–volume relationship. Moreover, a schematic representation of the helium porosimeter apparatus employed in this study is presented in **Fig. 3** [13]. All core samples were re-measured after acidizing to account for any minor dimensional change. Furthermore, the variation in diameter was less than 0.3 mm and had no measurable effect on the porosity results, as the Helium Porosimeter automatically adjusts for actual sample volume according to Boyle's law.

The porosities of the core samples were measured using a Helium Porosimeter (Iran, Petro Ahura). The porosity measurements were performed based on the Boyle's law principle, using high-purity helium gas as the displacement medium to ensure accurate pore-volume determination. The operating pressure range was maintained between 300 and 1000 psi, with a stabilization time of 25 seconds for each reading to achieve equilibrium. The instrument was calibrated using a reference aluminum standard prior to each set of measurements. In addition, porosity tests were conducted at ambient temperature (26 °C) under steady-state flow conditions. Each sample was tested three times, and the mean value was reported as the final porosity result. These

additions ensure transparency and reproducibility of the porosity measurements, enhancing the reliability of the reported data.

Fig. 3 A schematic of helium porosimeter device.

For the acidizing experiments, each carbonate core plug was first accurately weighed to record its initial mass. Afterwards, the samples were immersed in the prepared acidic solution under controlled laboratory conditions. At predetermined time intervals, the cores were removed, carefully washed and dried to eliminate excess acid, and subsequently reweighed. By comparing the recorded weights over time, the progressive mass reduction of the cores was quantified. These measurements were then used to construct a weight-loss profile, providing a clear representation of the dissolution kinetics and the efficiency of the acid–rock interaction during the treatment.

Results and Discussions

Core No. 15 – 15% HCl + Distilled Water (Oil-Free)

According to the **Figures 4 and 5**, Core 15 (12.719 g, 44.21% porosity) was treated with 15 wt.% HCl prepared with distilled water. The acid–rock reaction was extremely rapid at the start, reaching a dissolution rate of 1.157 g/min in the first minute, but the rate collapsed after three minutes, with only 0.052 g/min between 3–5 minutes. After 10 minutes, the rock lost 17.64% of its weight, but porosity decreased from 44.21% to 32.03%, showing that the process reduced flow capacity instead of improving it. The main mechanism was facing dissolution, where acid was consumed at the surface without penetrating deeper. Moreover, gas bubbles of CO_2 blocked reactive surfaces, and local pH increased, causing secondary calcite precipitation inside pore throats. In addition, the use of distilled water (low ionic strength) destabilized the double layer and promoted or intensified fines migration, which clogged pore constrictions. Furthermore, the combined effects of CO_2 coverage, precipitation, and fines plugging explain why porosity fell despite mineral removal. Moreover, from an engineering standpoint, this scenario highlights the inefficiency of DI water as a carrier fluid. Furthermore, to achieve wormhole formation, seawater or synthetic brines should be used, which provide ionic stability and prevent plugging. Moreover, retarded acids (HCl–acetic blends, emulsified or gelled acids) and proper pre-/post-flush brine stages are recommended. Without these measurements, DI-based acidizing leads to surface erosion, blocked pores, and poor stimulation efficiency.

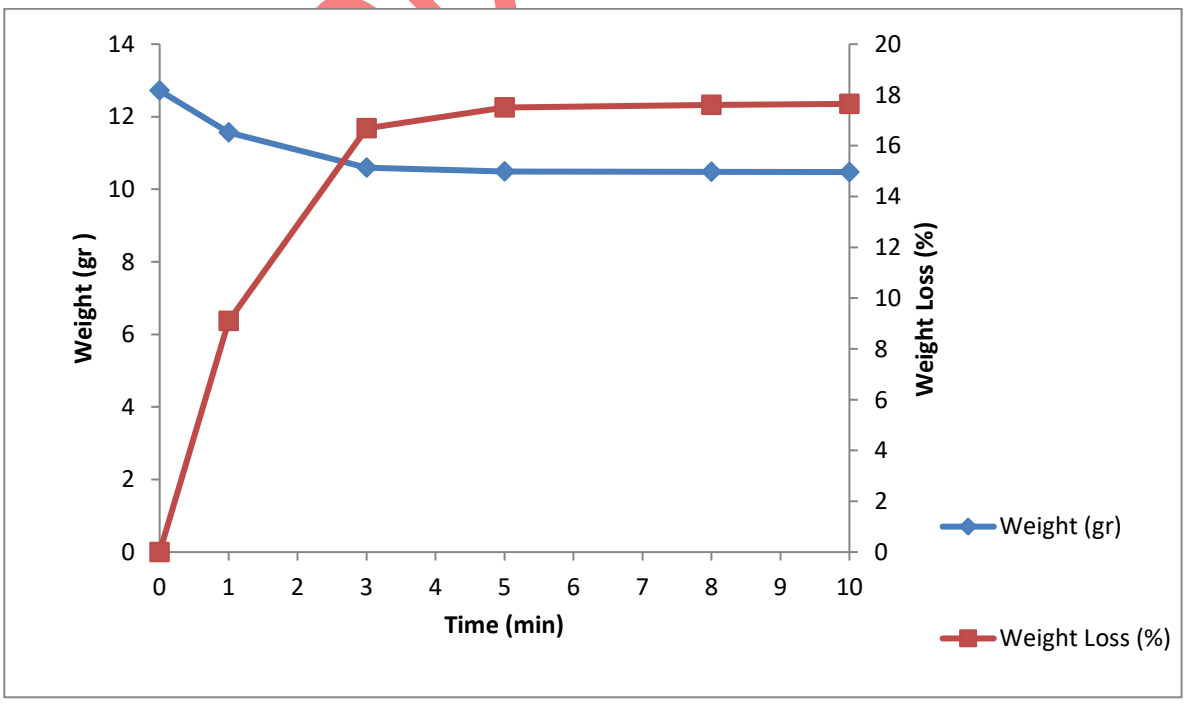

Fig 4. Weight reduction of Core 15 at different times in 15 wt.% hydrochloric acid solution with distilled water.

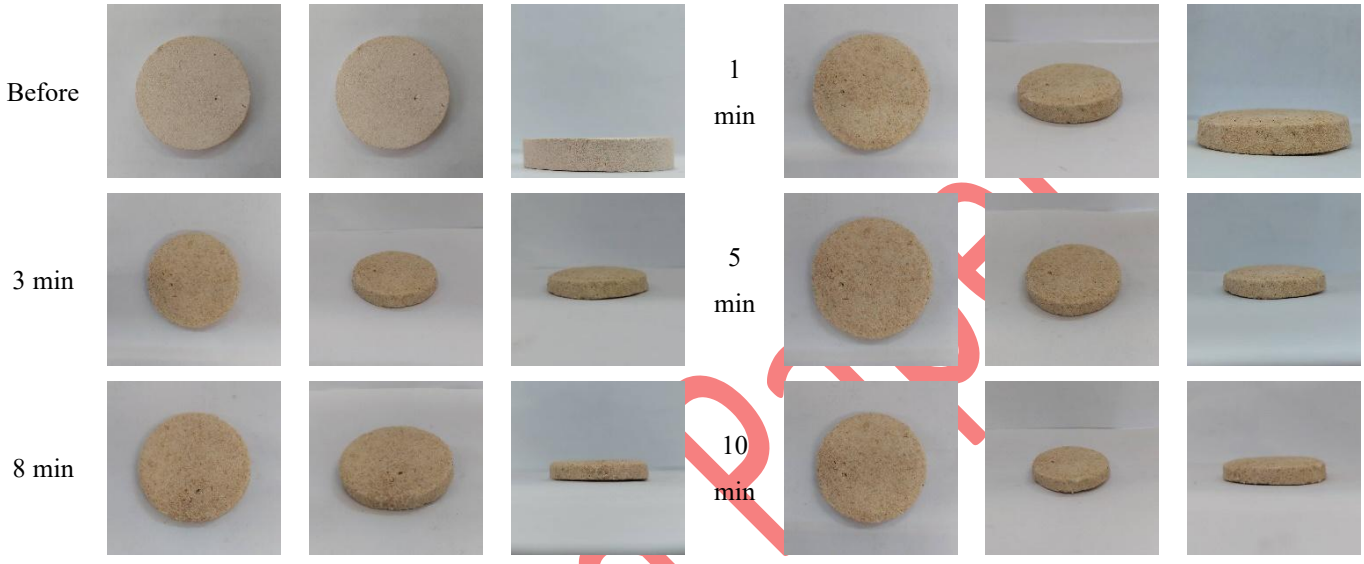

Fig. 5 Images of Core 15 at different time intervals after exposure to 15 wt.% hydrochloric acid solution with distilled water.

3.2 Core No. 16 – 15% HCl + Seawater (Oil-Free)

According to the **Figures 6 and 7**, Core 16 (16.132 g, 41.94% porosity) showed a more balanced and sustainable dissolution pattern when treated with 15 wt.% HCl in seawater. In the first minute, the dissolution rate was high (1.347 g/min) and remained significant over time, resulting in a 31.69% mass loss after 10 minutes. Unlike Core 15, porosity increased substantially to 50.04%, confirming that seawater helped maintain dissolution pathways. Mechanistically, the presence of Na^+, Mg^{2+}, and SO_4^{2-} ions stabilized the system, reduced the risk of secondary calcite precipitation, and improved acid transport into deeper regions of the core. The ionic strength of seawater also minimized fines detachment, keeping pore channels open. Instead of face dissolution, partial wormhole development was achieved, allowing connectivity and porosity growth. Compared with distilled water, seawater slowed down early acid spending and enhanced penetration depth. This highlights the critical role of carrier chemistry in carbonate acidizing. From an engineering perspective, seawater is a superior carrier fluid because it reduces precipitation, balances reaction kinetics, and promotes wormhole propagation. For field applications, this approach provides more sustainable stimulation efficiency and is recommended where natural brines are available.

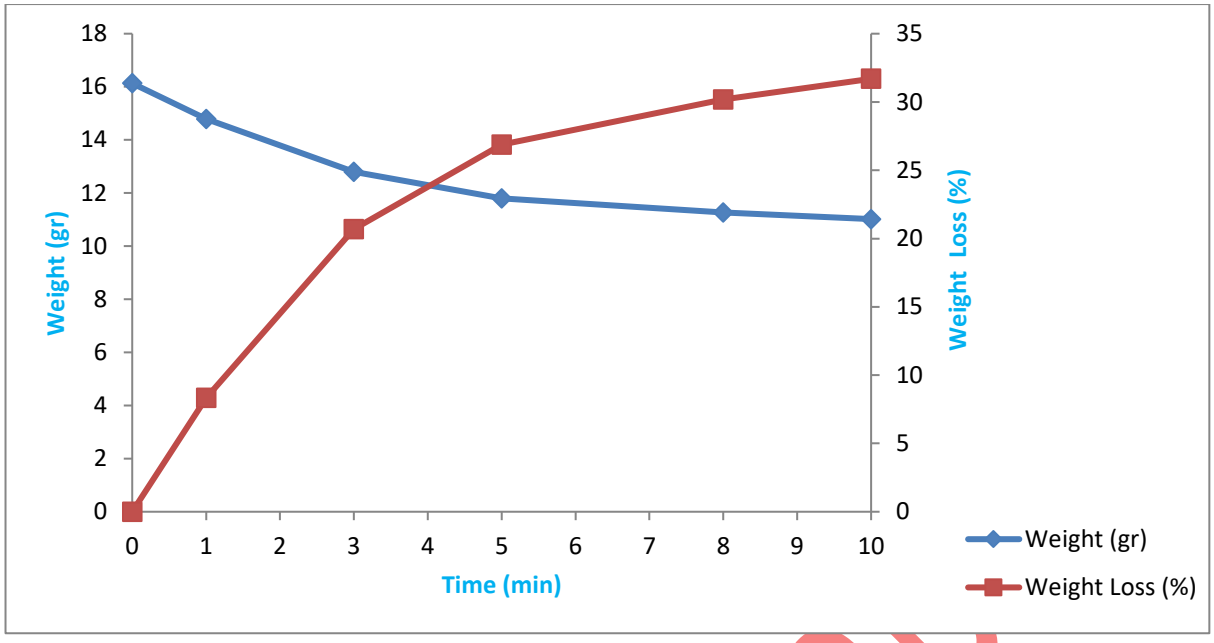

Fig. ۶ Weight reduction of Core 16 at different times in 15 wt.% hydrochloric acid solution with seawater.

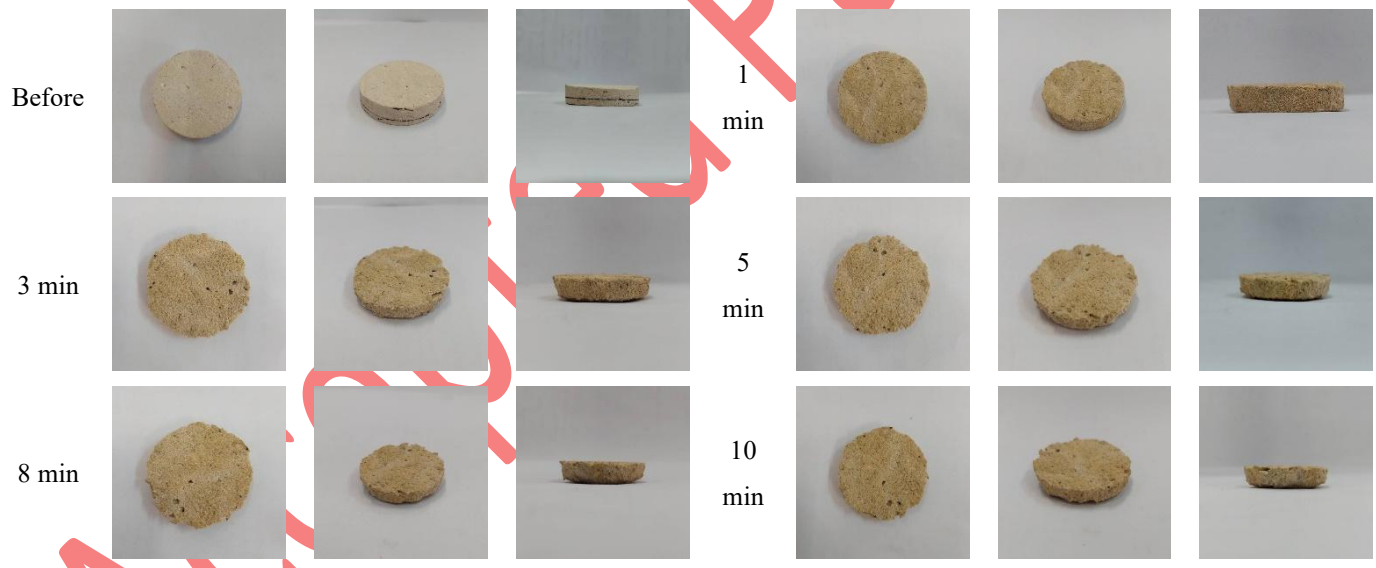

Fig. 7 The images of Core 16 at different time intervals after exposure to 15 wt.% hydrochloric acid solution with seawater.

Core No. 19 – 28% HCl + Distilled Water (Oil-Free)

According to the **Figures ٨ and ٩**, Core 19 (14.703 g, 47.05% porosity) was tested with 28 wt.% HCl in distilled water. The initial reaction was violent, producing a dissolution rate of 2.865 g/min in the first minute, but soon collapsed as acid was consumed at the surface. After 10 minutes, 26.47% of the core mass was dissolved, as the amount of porosity decreased slightly to 46.64%. The strong acid induced face dissolution, creating a saturated boundary layer of reaction products that blocked deeper acid penetration. Rapid CO_2 release covered reactive surfaces, and H^+ depletion raised pH, driving secondary mineral precipitation. In DI water, the lack of ionic stability promoted fines migration; and thereby, pores are blocked. The net result was a significant mass removal but ineffective porosity improvement. Mechanistically, this represents uncontrolled kinetics without transport balance. From an engineering perspective, using concentrated HCl with DI water is counterproductive; it causes (1) surface erosion, (2) plugging, and (3) wasted acid. To achieve wormholes, retardation techniques or ionic carriers (seawater, synthetic brines) must be applied. Otherwise, stimulation fails, and reservoir damage may result.

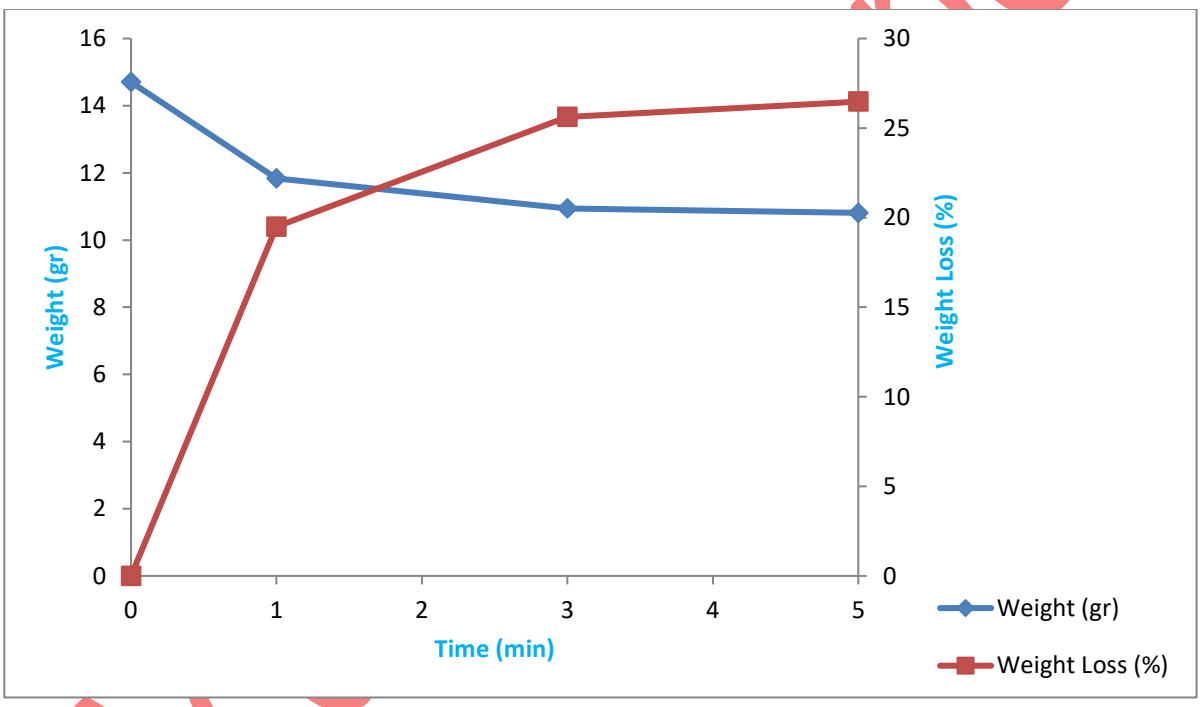

Fig ٨. Weight reduction of Core 19 at different times in 28 wt.% hydrochloric acid solution with distilled water.

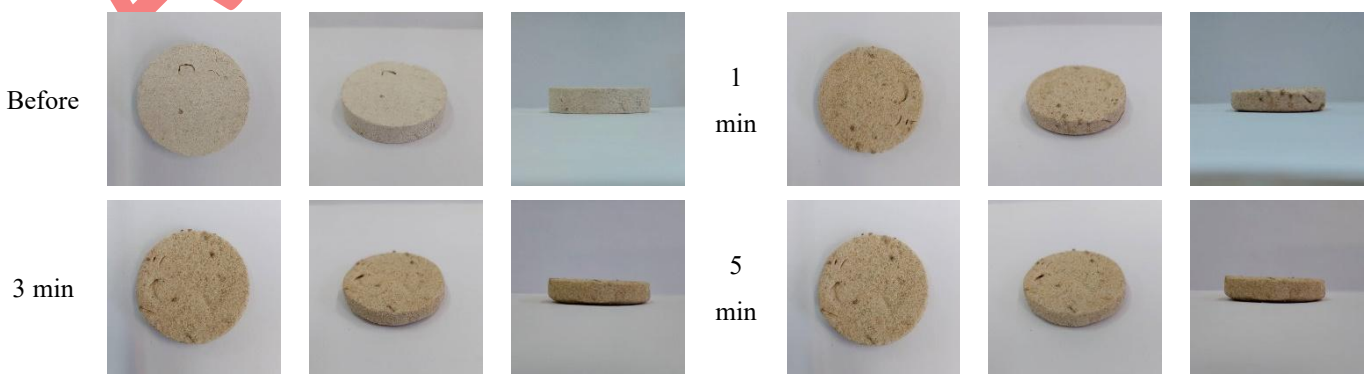

Fig 9. Images of Core 19 at different time intervals after exposure to 28 wt.% hydrochloric acid solution with distilled water.

Core No. 21 – 28% HCl + Seawater (Oil-Free)

According to the **Figures 10 and 11,** Core 21 (14.115 g, 48.75% porosity) produced the most efficient response **among** all tests. Treated with 28 wt.% HCl in seawater, the core lost 78.87% of its weight, and porosity increased dramatically to 86.13%. Dissolution was vigorous and sustained, with a rate of 3.924 g/min in the first minute and still 0.354 g/min after 10 minutes, which it proves continuous

reactivity. Mechanistically, the high acid concentration ensured strong dissolution capacity, while seawater ions stabilized the environment, prevented premature precipitation, and maintained transport pathways. This created ideal conditions for wormhole formation, with deep, connected channels that drastically enhanced porosity. Unlike the DI water case (Core 19), where dissolution was limited to the surface, seawater enabled full propagation of acid flow paths. From an engineering viewpoint, this represents an optimal acidizing scenario. In practice, however, concentrated HCl requires corrosion inhibitors and anti-sludge additives to manage risks. Still, Core 21 highlights that seawater combined with high HCl strength can maximize stimulation efficiency, making it a benchmark for carbonate acidizing strategies. The conical and cleft-like geometries observed in the acidized cores are attributed to the higher dissolution rate near the acid-inlet region and progressive depletion of acid strength along the core length, as well as localized channeling caused by preferential flow paths and CO_2 gas evolution.

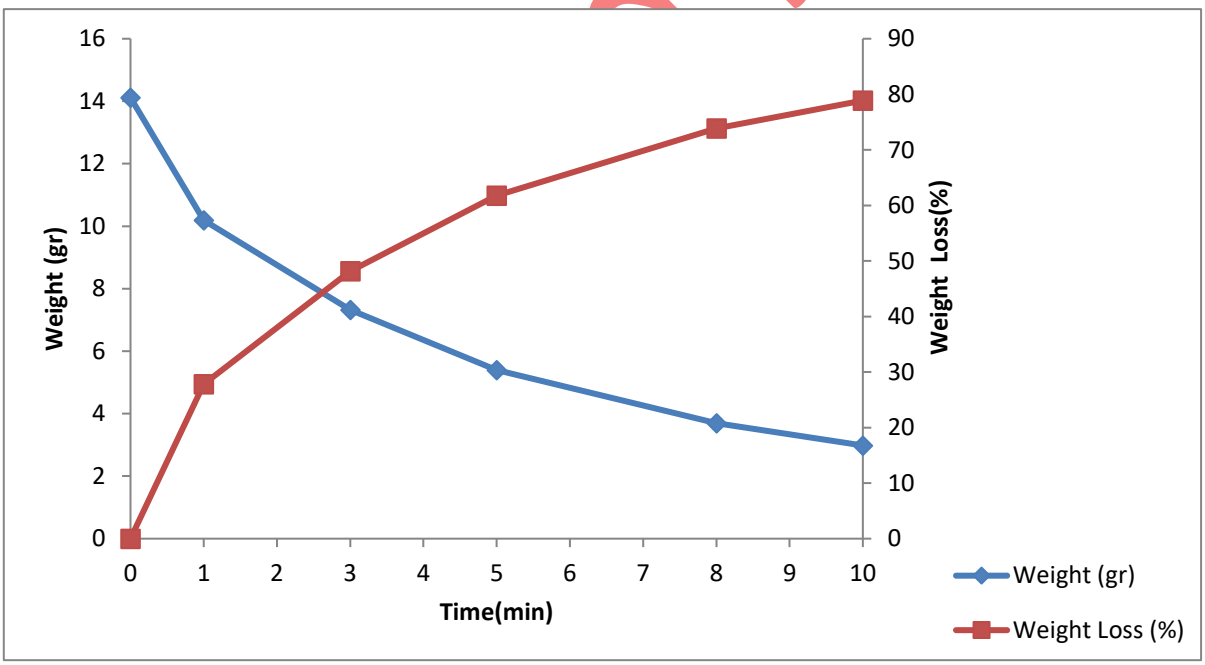

Fig 10. Weight reduction of Core 21 at different times in 28 wt.% hydrochloric acid solution with seawater.

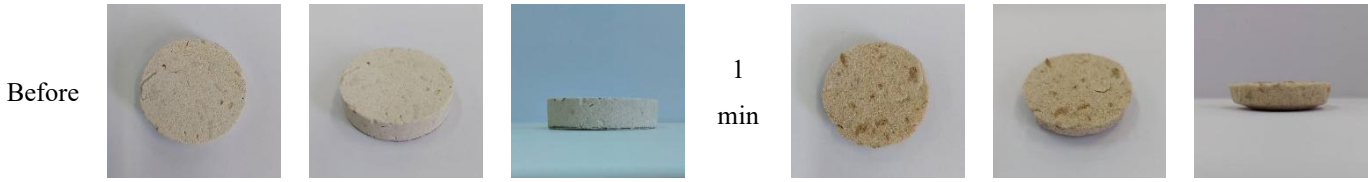

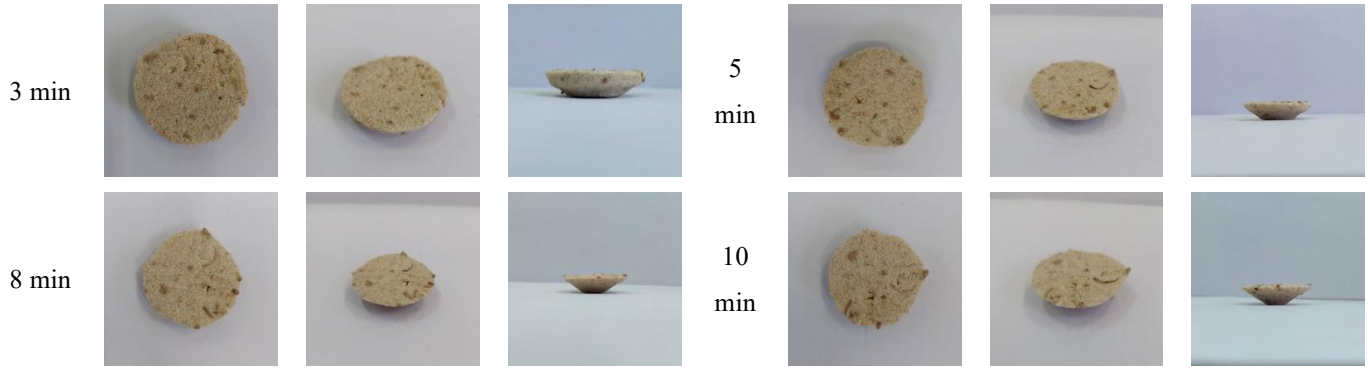

Fig 11. Images of Core 21 at different time intervals after exposure to 28 wt.% hydrochloric acid solution with seawater.

Core No. 17 – 15% HCl + 3% Acetic Acid + Seawater (Oil-Free)

According to **the Figures 12 and 13,** Core 17 (12.856 g, 43.70% porosity) was treated with a mixture of 15 wt.% HCl and 3 wt.% acetic acid in seawater. The dissolution profile was smoother, with an initial rate of 1.052 g/min,

decreasing gradually instead of collapsing, and achieving 49.33% weight loss with porosity increasing to 59.27%. Moreover, the acetic acid acted as a retarder, slowing the kinetics of HCl, preventing rapid surface reaction, and allowing the acid to penetrate deeper. Furthermore, the presence of seawater ions further enhanced the dissolution process by suppressing secondary precipitation and stabilizing fine particles. The result was more uniform dissolution and partial wormhole development, rather than surface-limited erosion. Also, mechanistically, the balance between strong mineral dissolution (HCl) and controlled kinetics (acetic acid) optimized reactivity and transport. From an engineering perspective, this demonstrates the benefit of blended acid systems: they (1) extend acid effectiveness, (2) improve depth of treatment, and (3) reduce risk of near-wellbore plugging. Such systems are recommended where conventional HCl treatments risk early acid spending or formation damage.

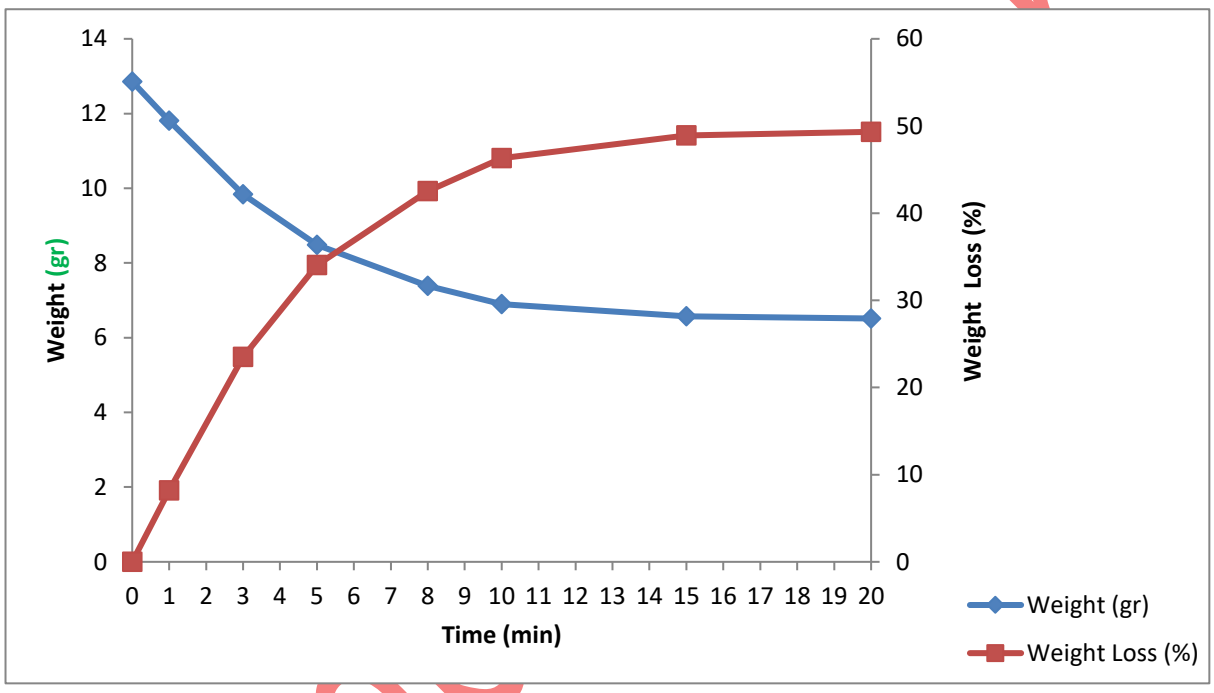

Fig 12 . Weight reduction of Core 17 at different times in 15 wt.% hydrochloric acid and 3 wt.% acetic acid solution with seawater.

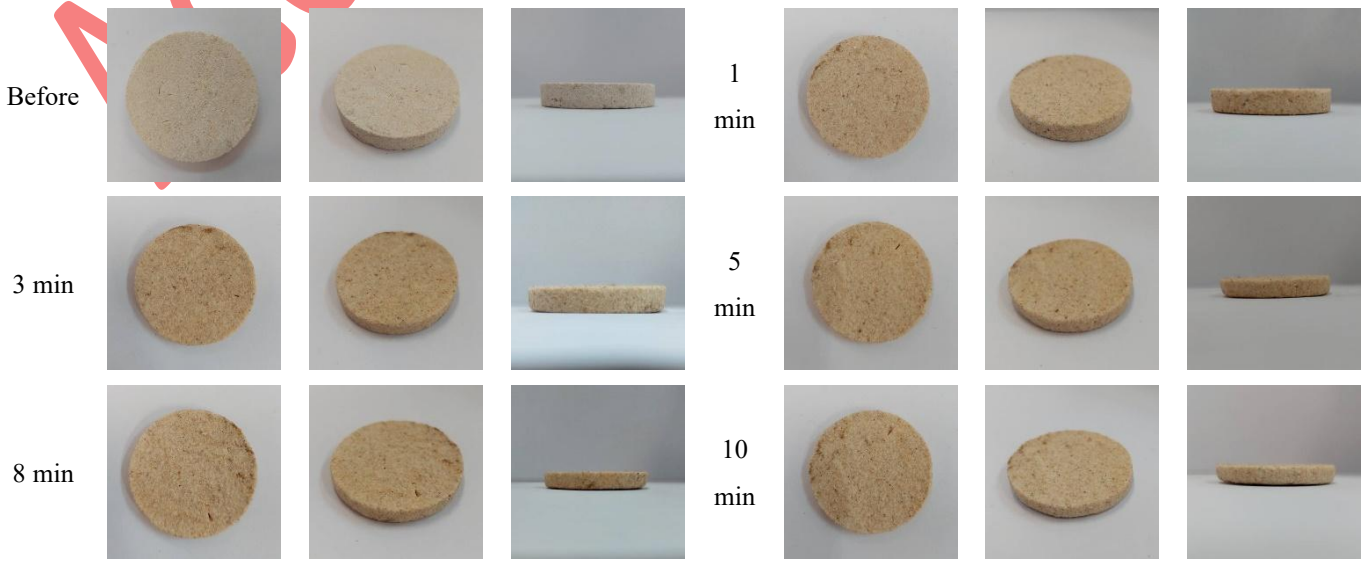

15 min    20 min   

Fig 13. Images of Core 17 at different time intervals after exposure to 15 wt.% hydrochloric acid and 3 wt.% acetic acid solution with seawater.

Core No. 7 – 28% HCl + Distilled Water (Oil-Saturated)

According to the **Figures 14 and 15**, Core 7 (16.067 g, 45.48% porosity), saturated with oil, showed poor acidizing response when treated with 28 wt.% HCl in distilled water. The first minute dissolved 0.979 g, but

activity quickly declined. After 10 minutes, only 17.87% weight loss was achieved, and porosity collapsed to 17.50%. The key issue was acid sludge formation: strong HCl destabilized asphaltenes and resins in crude oil, producing insoluble sludge that blocked pores. The injection of deionized water promotes the migration of fine particles, thereby inducing severe pore-throat clogging. Moreover, CO_2 bubble coverage and local precipitation further worsened the situation. Furthermore, mechanistically, the reaction failed due to incompatibility between acid and crude oil. From an engineering standpoint, this scenario represents a high-risk operation: DI water and strong HCl in oil-bearing formations cause irreversible damage. Field practice must use seawater or brines as carriers, add anti-sludge additives, and include pre-flush surfactants to alter wettability and minimize sludge risk.

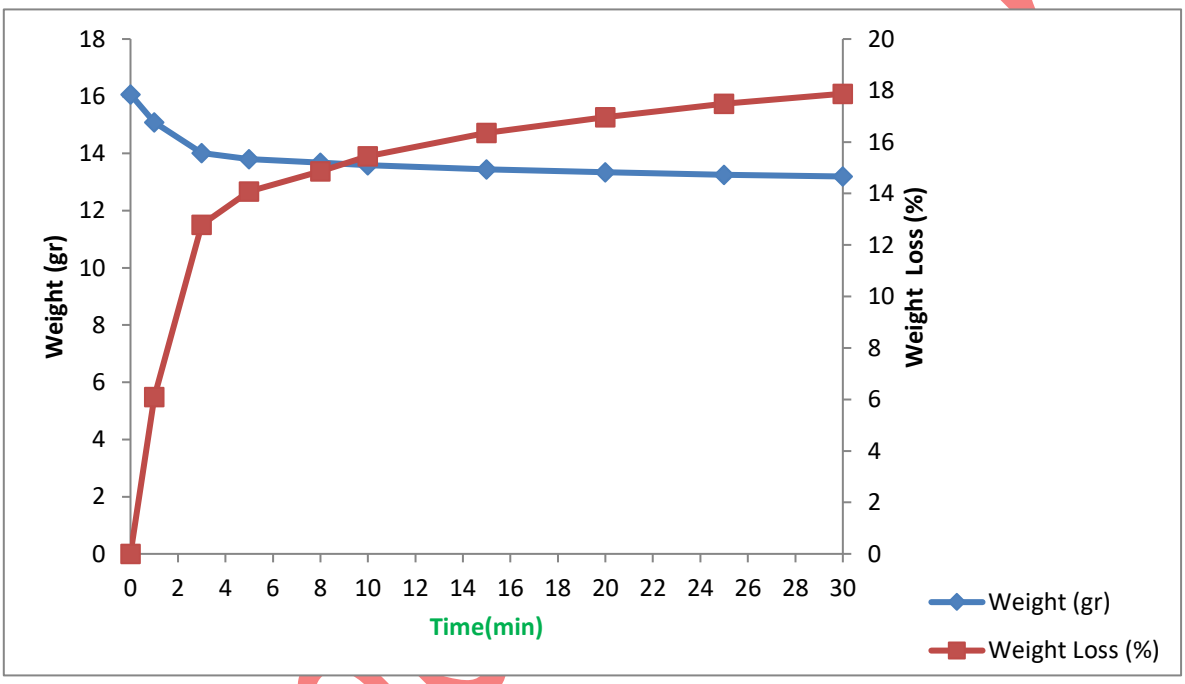

Fig 14 . Weight reduction of Core 7 at different times in 28 wt.% hydrochloric acid solution with distilled water.

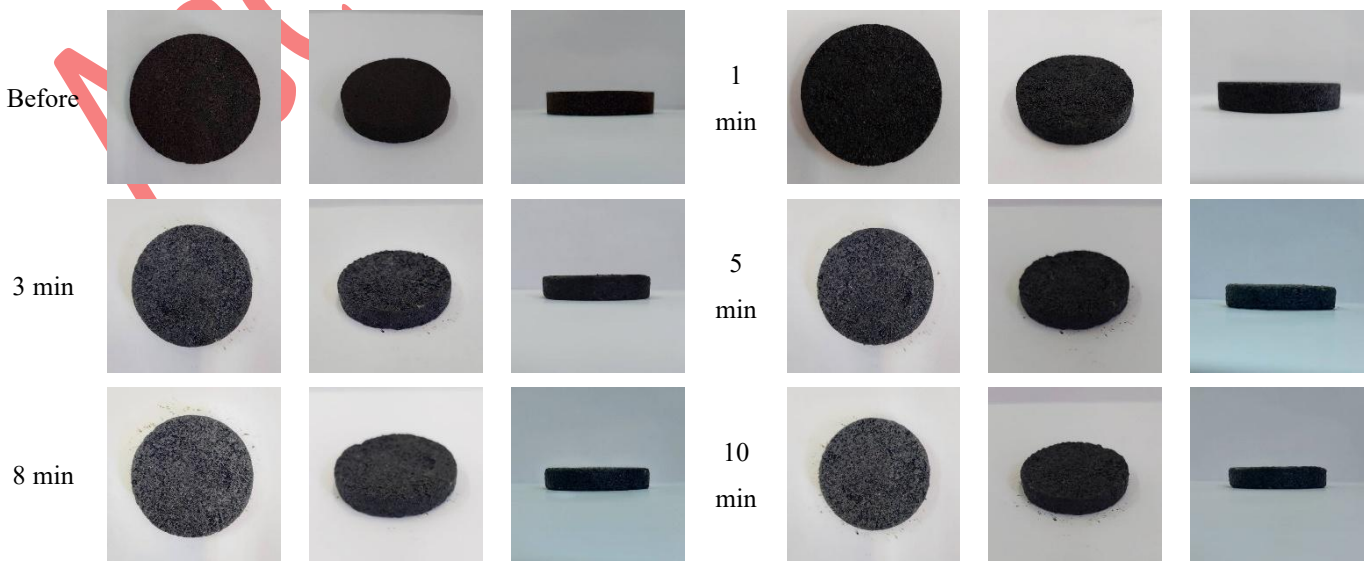

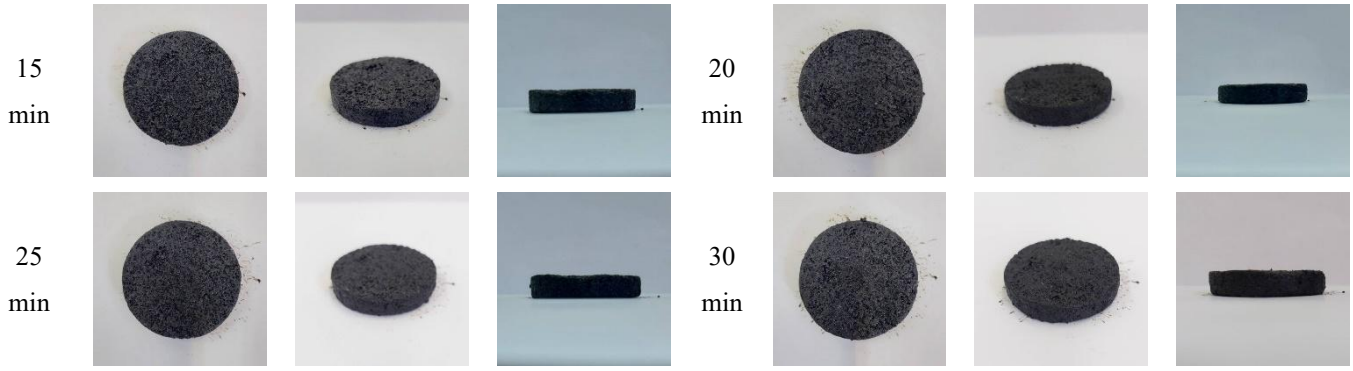

Fig 15. Images of Core 7 at different time intervals after exposure to 28 wt.% hydrochloric acid solution with distilled water.

Core No. 9 – 28% HCl + Seawater (Oil-Saturated)

According to the **Figures 16 and 17**, Core 9 (15.727 g, 42.52% porosity) delivered strong results when treated with 28 wt.% HCl in seawater. Dissolution was sustained over 30 minutes, with 60.37% weight loss and porosity rising to 59.85%. Unlike Core 7, where sludge blocked pores, seawater ions stabilized crude oil organics and suppressed sludge formation. Moreover, this enabled continuous reactivity, deep acid penetration, and wormhole-like channel development. Furthermore, CO_2 bubbles were less problematic because ionic stabilization improved bubble detachment and transport. In addition, mechanistically, the combination of strong acid capacity and seawater chemistry produced efficient dissolution even in an oil-wet environment. From an engineering perspective, this proves that seawater is essential for safe acidizing of oil-bearing carbonates. With inhibitors and additives, this system can achieve reliable stimulation, preventing sludge and enhancing flow capacity. Core 9 demonstrates the decisive role of carrier fluid chemistry in determining acidizing success under real reservoir conditions.

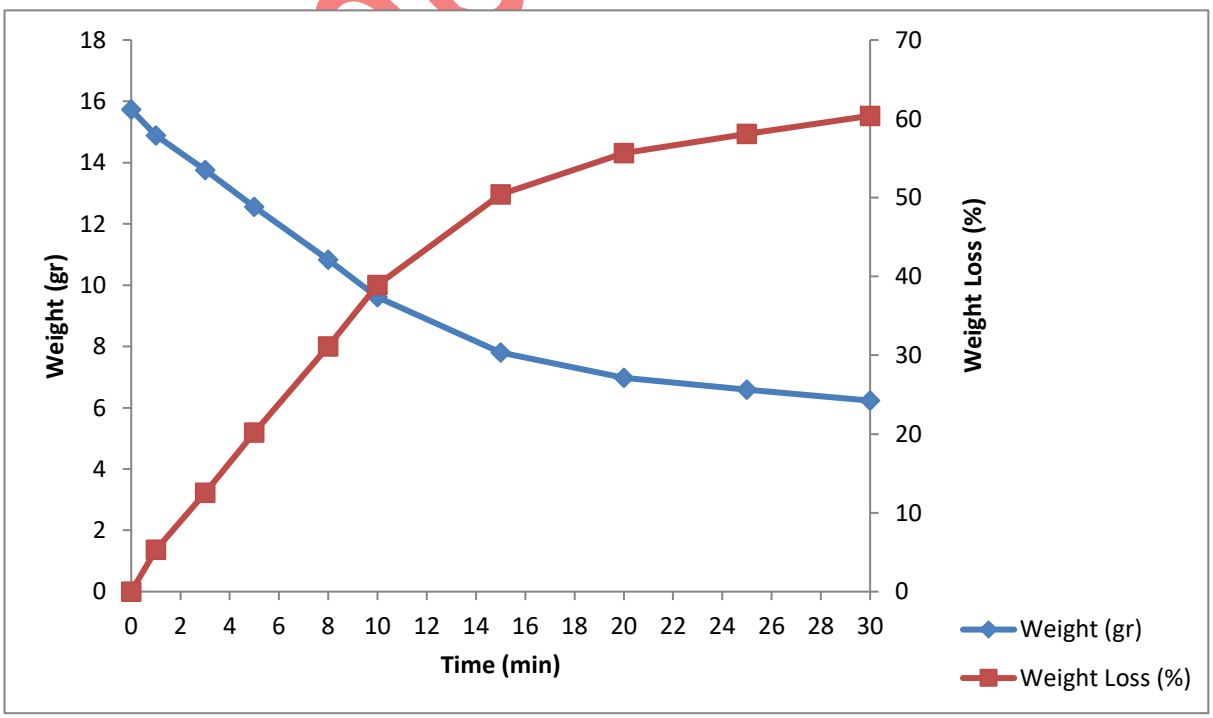

Fig 16. Weight reduction of Core 9 at different times in 28 wt.% hydrochloric acid solution with seawater.

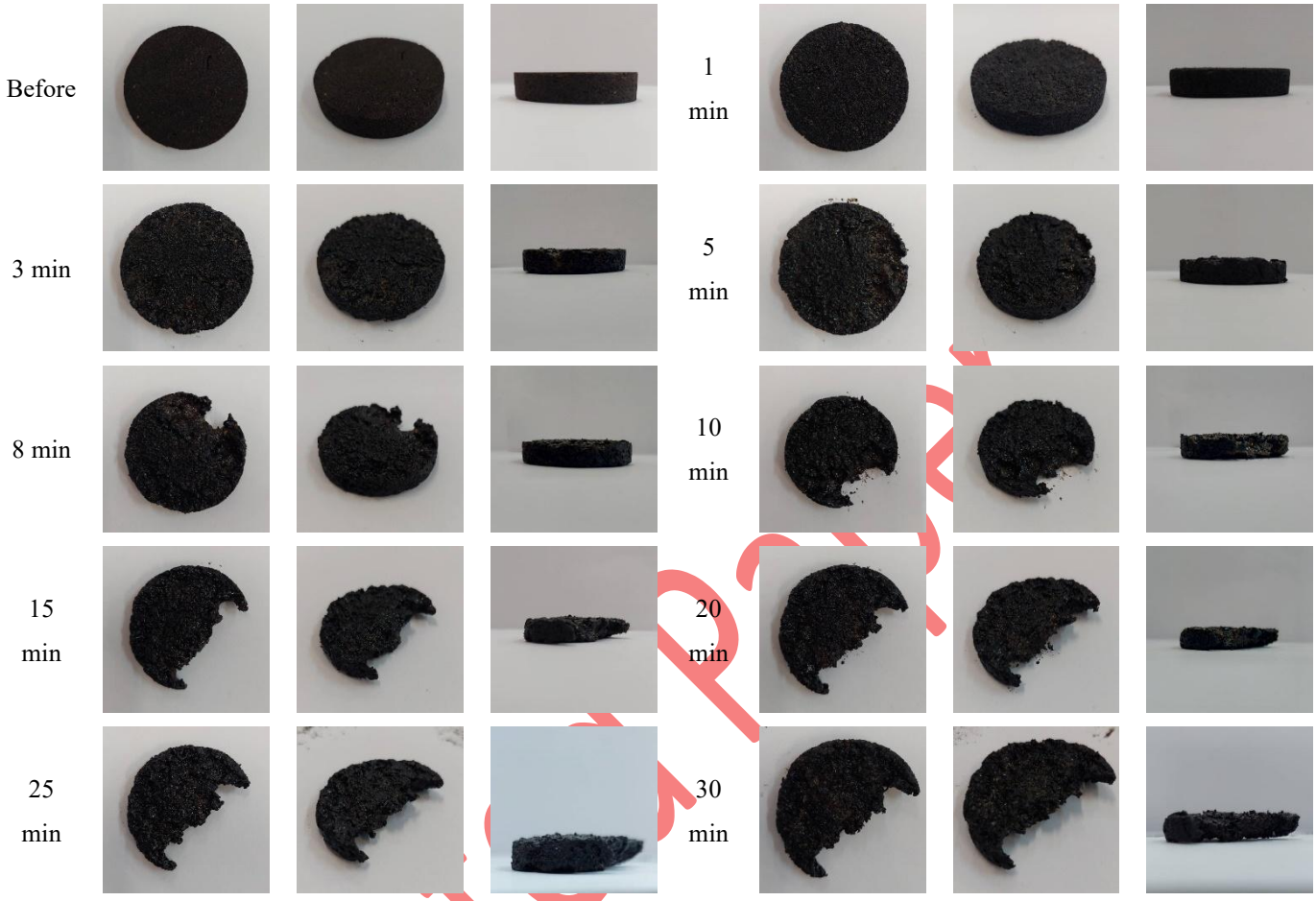

Fig 17. Images of Core 9 at different time intervals after exposure to 28 wt.% hydrochloric acid solution with seawater.

Core No. 5 - 28% HCl + seawater after contact with surfactant solution

According to the **Figures 18 and 19,** Core No. 5 was pre-treated with a CTAB surfactant solution (500 ppm in seawater, 120 min at 70 °C) to alter wettability and enhance acid–rock contact. Then it was subjected to 28 wt.% HCl prepared with seawater, with dissolution behavior monitored at different intervals. The initial weight and porosity were 17.6381 g and 47.34%, respectively. The reaction began vigorously, with a dissolution rate of 1.6835 g/min in the first minute, but decreased rapidly thereafter to 0.3235 g/min (1–3 min), 0.2159 g/min (3–5 min), 0.1121 g/min (5–8 min), and stabilized at 0.0354 g/min after 10 minutes. In total, 21.49% of the core mass was removed. Unexpectedly, porosity decreased to 22.77%, indicating surface-limited face dissolution rather than wormhole development. This outcome was attributed to CO_2 bubble accumulation hindering acid penetration, secondary calcite precipitation caused by localized pH increase, and acid sludge formation from destabilized organics, all of which blocked pore throats and reduced flow pathways. Despite substantial mineral dissolution, stimulation efficiency remained low, accompanied by a reduction in overall flow capacity. These results underscore the importance of using retarded acids, anti-sludge additives, and optimized brine pre- and post-flush sequences to properly balance reaction kinetics and transport dynamics, ensuring sustainable wormhole development in carbonate formations.

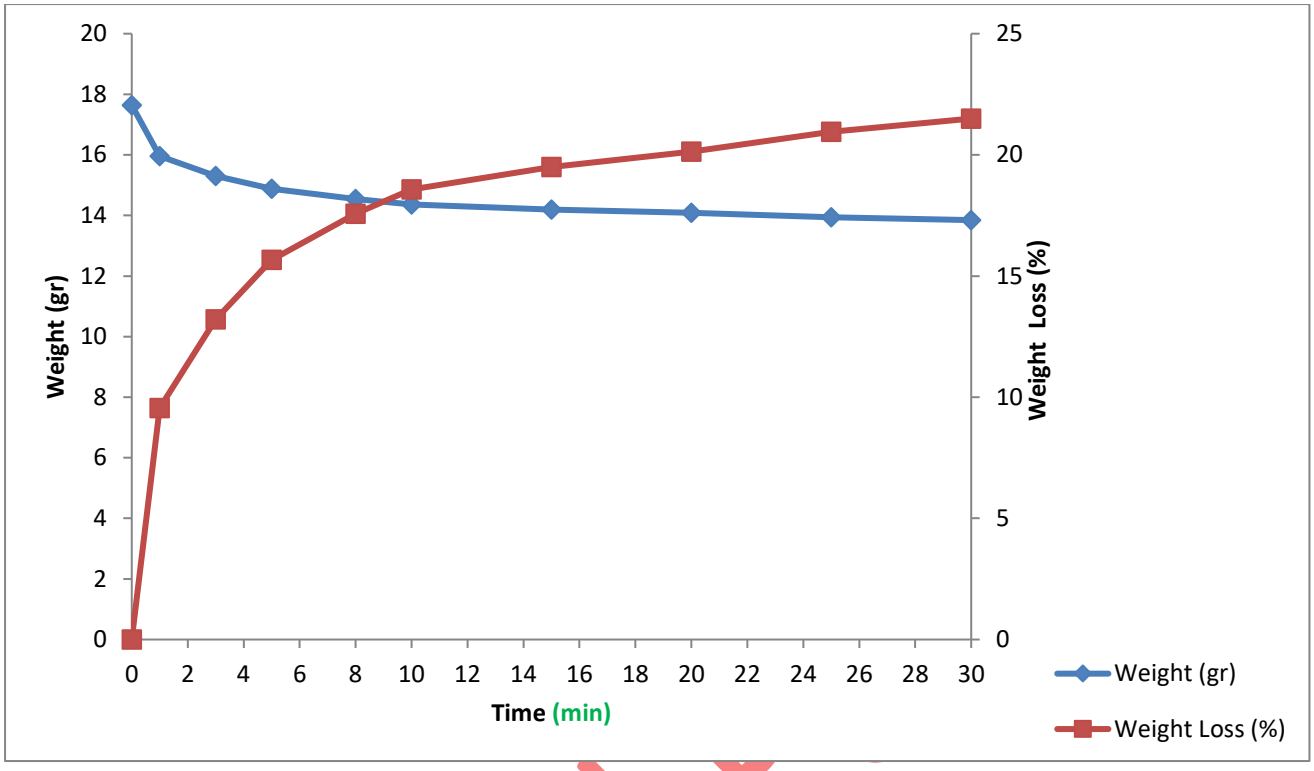

Fig 18 . Weight loss of core 5 at different times in 28% by weight hydrochloric acid solution and seawater after mixing with surfactant.

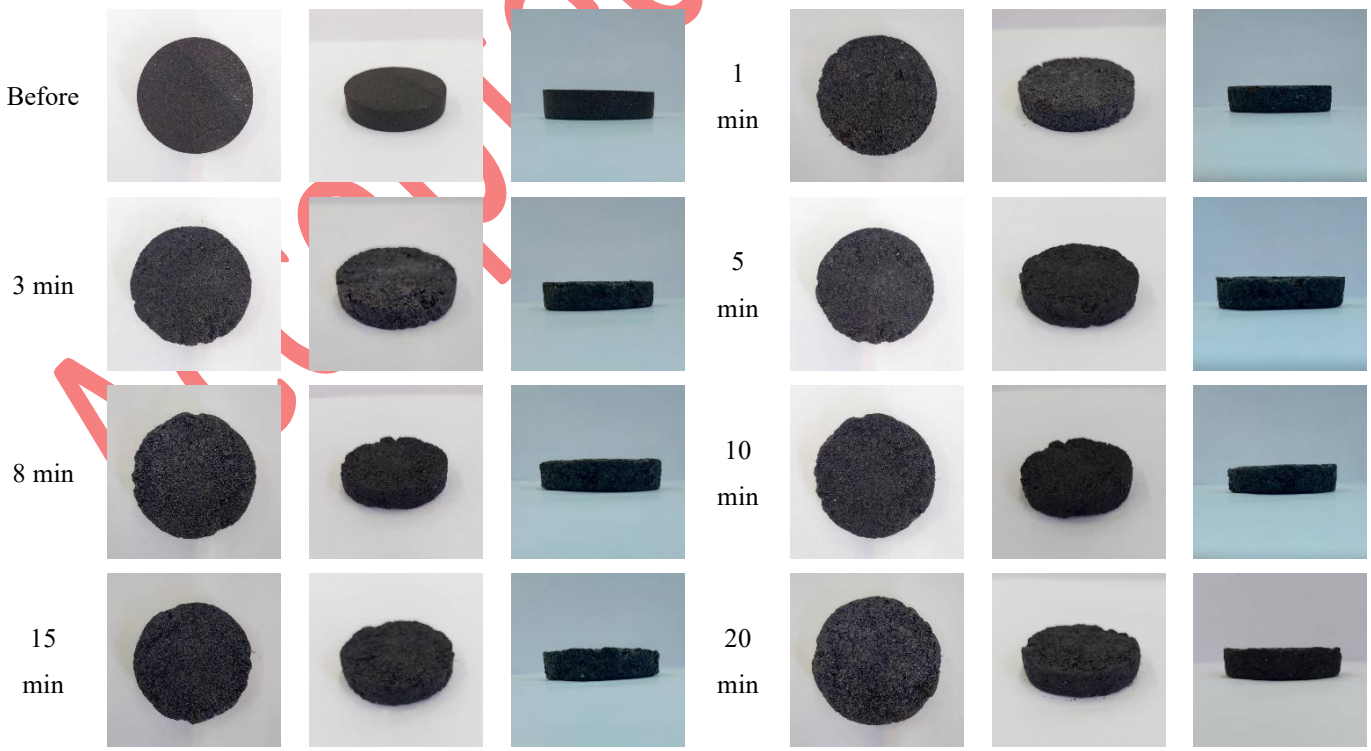

25 min  30 min 

Fig 19. Images of core 5 at different time intervals after contact with 28% by weight hydrochloric acid solution with seawater after mixing with surfactant.

Core No. 3 - 28% HCl + Distilled Water after Contact with Surfactant Solution

According to the **Figures 20 and 21**, Core No. 3 was initially conditioned with a CTAB surfactant solution (500 ppm in seawater) for 120 minutes at 70 °C to modify wettability and enhance subsequent acid–rock interaction. The core was then exposed to a 28 wt.% hydrochloric acid solution prepared with distilled water, and weight changes were monitored over time. The initial core weight was 17.0763 g, with a porosity of 45.583%. The acid–rock reaction began with extremely high intensity, recording a dissolution rate of 3.3054 g/min in the first minute. However, the rapid surface reaction consumed the acid quickly, causing the dissolution rate to decline sharply to 0.9957 g/min during 1–3 minutes and to approach a nearly stable value after 10–15 minutes, indicating loss of

acid reactivity. Overall, only 1.43% of the core's initial weight was dissolved, while final porosity decreased slightly to 44.856%. Moreover, these findings confirm that the dominant mechanism was surface-limited face dissolution, where acid was consumed near the surface and failed to penetrate deeper into the core to create wormhole channels. Contributing factors included CO_2 bubble accumulation that blocked reactive sites, secondary calcite precipitation due to localized pH rise, and lack of ionic stabilization because distilled water was used instead of seawater. Consequently, despite the vigorous initial reaction, overall stimulation efficiency was poor and flow capacity was not improved. From an engineering perspective, using ionic carriers such as seawater or synthetic brines, together with retarded acids and anti-sludge/anti-precipitation additives, would promote deeper penetration, wormhole formation, and more effective carbonate acidizing under such conditions. Furthermore, the total weight loss of the core after 30 minutes of acidizing was 4.17% of the initial mass, while the early-stage (5 min) dissolution accounted for approximately 1.43%. Moreover, the initially reported 1.43% value represented the partial weight loss during the early phase of reaction rather than the total mass reduction." Also, this clarification ensures accuracy, avoids ambiguity, and confirms that the value of 1.43% was not an error but a time-specific measurement within the overall dissolution process.

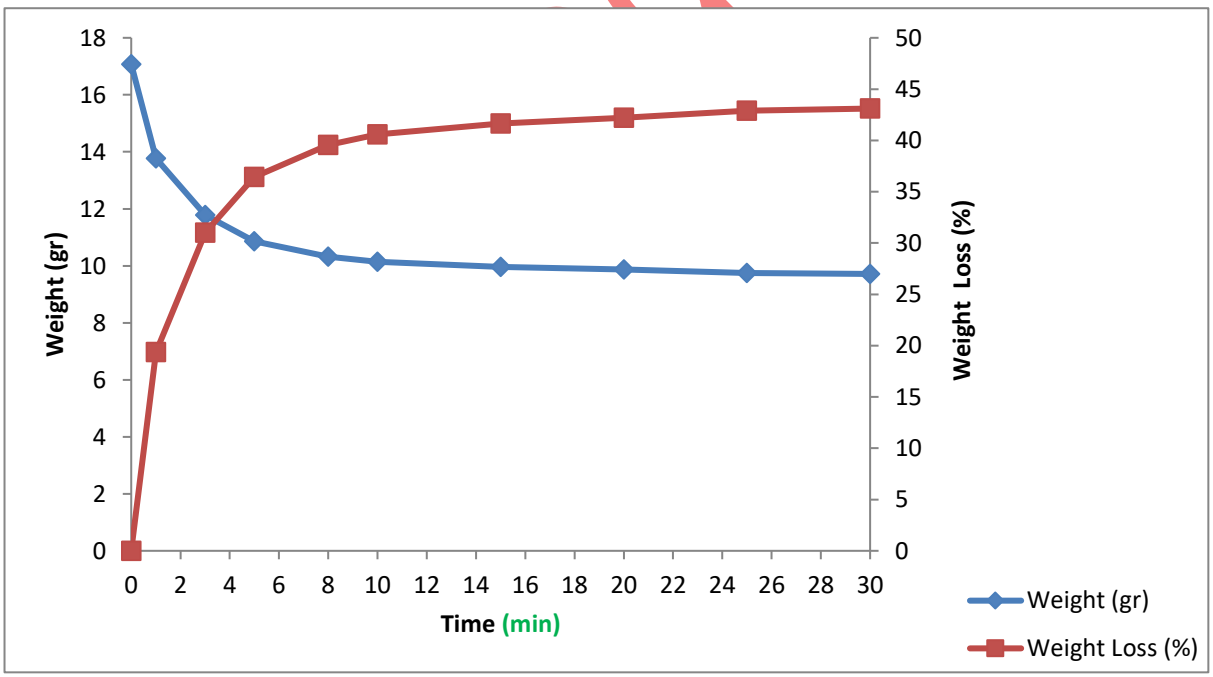

Fig 20. Weight loss of core 3 at different times in 28% by weight hydrochloric acid solution and distilled water after contact with surfactant solution.

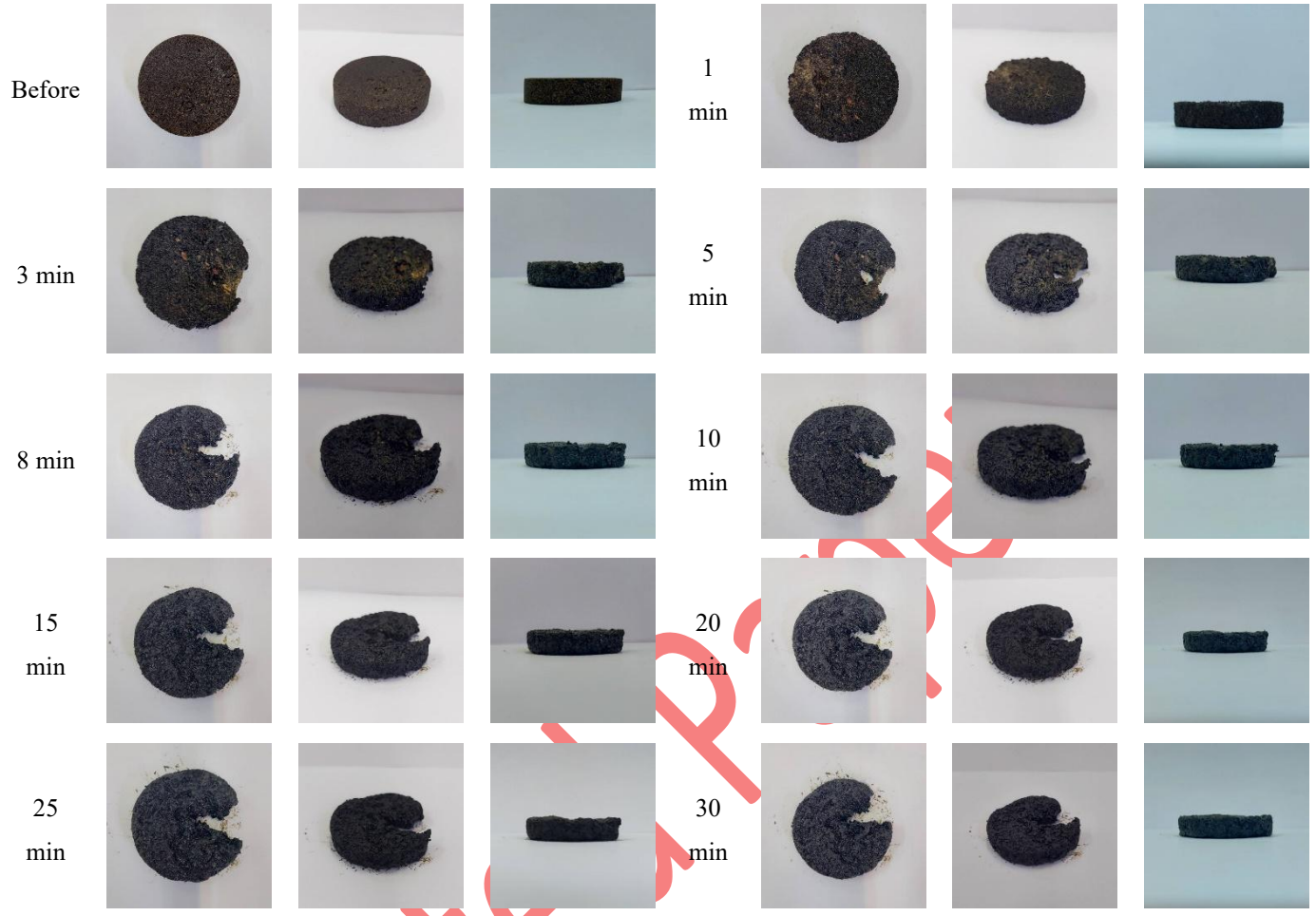

Fig 21. Images of core 3 at different time intervals after contact with 28% by weight hydrochloric acid solution with distilled water after contact with surfactant solution.

The present study primarily focuses on the effects of acid type, concentration, and carrier-fluid composition. Moreover, investigation of additional variables such as temperature and flow rate, and derivation of complete kinetic correlations, are proposed for future work. In this study, the verification of wormhole formation was based mainly on porosity enhancement and dissolution data. Furthermore, further microscopic and imaging analyses are planned for future work to provide more direct structural evidence.

Conclusions

In this study, the dissolution kinetics and porosity enhancement of carbonate cores were investigated under various acidizing conditions. The results confirmed that the efficiency of stimulation is strongly dependent on the chemistry of the carrier fluid, the acid concentration, and wettability alteration strategies.

1- Distilled water as the carrier fluid caused severe face dissolution, secondary calcite precipitation, fines migration, and pore blockage, ultimately reducing porosity. In contrast, seawater provided ionic stability, suppressed precipitation, and enabled wormhole development with significant porosity growth.

2- Stimulation with high-strength HCl (28 wt.%) in seawater proved most effective, yielding nearly 79% weight loss and an 86% increase in porosity. The same acid concentration in distilled water was counterproductive; therefore, it leads (1) surface erosion and (2) inefficient acid consumption.

3- A blended acid system of 15 wt.% HCl with 3 wt.% acetic acid in seawater achieved (1) smoother kinetics, (2) deeper penetration, and (3) more uniform dissolution; and thereby, the risk of near-wellbore plugging is reduced.

4- Under oil-saturated conditions, distilled water promoted or intensified sludge formation from destabilized asphaltenes, collapsing porosity, whereas seawater suppressed sludge formation, sustained reactivity, and allowed porosity to rise significantly.

As discussed in Section 3 (Results and Discussion), the dissolution and porosity evolution trends observed in this study are in strong agreement with the established acid–rock interaction mechanisms described[17,18]. Specifically, our results confirm that optimum stimulation occurs in the intermediate regime between rapid face dissolution and slow uniform dissolution, which is characterized by stable wormhole development a finding also supported by these works.

Moreover, the improved performance of seawater-based acid systems observed in our experiments is consistent with the ionic interaction effects described by Rashid et al. in 2015, Nande et al. in 2021, and Buriro et al. in 2024, who showed that divalent ions such as Mg^{2+} and Ca^{2+} stabilize acid–rock reactions and enhance wormhole propagation. Similarly, the observed reduction in sludge formation in seawater-based systems under oil-saturated conditions agrees with the findings of Asaadian et al. in 2022 and Kalhori et al. in 2025, who reported that ionic strength and surfactant-assisted systems suppress asphaltene precipitation and maintain reactivity **[22,23,29,30,31].**

Therefore, both the dissolution kinetics and acidizing efficiency trends obtained in the present work are consistent with, and extend, the conclusions of prior studies in the literature, confirming the reliability and reproducibility of our experimental results.

Overall, the findings demonstrate that seawater-based carriers, especially when combined with high-strength HCl and proper additives, represent the optimal strategy for carbonate acidizing. This approach ensures sustainable wormhole formation, enhances conductivity, and provides a reliable framework for field-scale stimulation design.

Nomenclatures

CTAB: Cetyltrimethylammonium bromide

DI (Water): Deionized (water)

HCl: Hydrochloric acid

IFT: Interfacial tension

XRD: X-ray diffraction

XRF: X-ray fluorescence

References

[1] Garrouch, A. A., & Jennings Jr, A. R. (2017). A contemporary approach to carbonate matrix acidizing. *Journal of Petroleum Science and Engineering*, *158*, 129-143. doi.org/10.1016/j.petrol.2017.08.045 .

[2] Tanhaei, H., Dehaghani, A. H. S., & Motlagh, M. A. B. (2024). A Review of waste management approaches to maximise sustainable value of waste from the oil and gas industry. In The 2nd National and 1st International Conference on Environmental Challenges (Tarbiat Modares University, 2024). https://civilica.com/doc/2034996.

[3] Wu, Y., Luo, W., Jia, X., Fang, H., Wang, H., & Yu, S. (2019). Application of VES acid system on carbonate rocks with uninvaded matrix for acid etching and fracture propagation. Processes, 7(3), 159. https://doi.org/10.3390/pr7030159.

[4] Yoo, H., Kim, Y., Lee, W., & Lee, J. (2018). An experimental study on acid-rock reaction kinetics using dolomite in carbonate acidizing. Journal of Petroleum Science and Engineering, 168, 478-494. doi: 10.1016/j.petrol.2018.05.041.

[5] Fan, Y., Peng, H., Chen, G., Peng, J., Han, H., Qin, Y., Wang, L. and Liu, D. (2023). Experimental study of the influences of different factors on the acid-rock reaction rate of carbonate rocks. Journal of Energy Storage, 63, 107064. https://doi.org/10.1016/j.est.2023.107064.

[6] Dehaghani, A. S., & Motlagh, M. B. (2025). Experimental investigation of foam stability under various salinity levels, oil types, and surfactant conditions: Effect of natural polymer lignin. Scientia Iranica. 10.24200/sci.2025.66165.9885.

[7] Parandeh, M., Dehkohneh, H. Z., & Soulgani, B. S. (2023). Experimental investigation of the acidizing effects on the mechanical properties of carbonated rocks. Geoenergy science and engineering, 222, 211447. doi.org/10.1016/j.geoen.2023.211447 .

[8] Yoo, H., & Lee, J. (2019). An experimental study on the optimum injection rate for matrix acidizing in carbonate reservoirs. Journal of the Korean Society of Mineral and Energy Resources Engineers, 56(3), 227-238. doi: 10.32390/ksmer.2019.56.3.227.

[9] Abass, H. H., Al-Mulhem, A. A., Alqam, M. S., & Mirajuddin, K. R. (2006, September). Acid fracturing or proppant fracturing in carbonate formation? A rock mechanic's view. In SPE Annual Technical Conference and Exhibition? (pp. SPE-102590). SPE. https://doi.org/10.2118/102590-MS.

[10] Karimi, M., Shirazi, M. M., & Ayatollahi, S. (2018). Investigating the effects of rock and fluid properties in Iranian carbonate matrix acidizing during pre-flush stage. Journal of Petroleum Science and Engineering, 166, 121-130. https://doi.org/10.1016/j.petrol.2018.03.002.

[11] Ahmadi, A., Paydar, K., Ebadi, A., & Manteghian, M. (2022). Study and Optimization of the Effect of Temperature, Acid Concentration, and Rock Grain Size on the pH of Carbonate Reservoir Acidizing. Journal of Chemical & Petroleum Engineering, 56(2), 331. https://doi.org/10.22059/jchpe.2022.342154.1391.

[12] Tanhaei, H., Saeedi Dehaghani, A. H., & Karami, S. (2025). Investigation of microwave radiation in conjugate with acidizing as a novel hybrid method of oil well stimulation. Scientia Iranica, 32(9). 10.24200/sci.2023.62586.7985.

[13] Rigi, E., Saeedi Dehaghani, A. H., & Sadeghnejad, S. (2025). The Effect of Wettability Alteration of Carbonate Rock Using Cetyltrimethyl Ammonium Bromide on Acidizing with HCl 15%. Journal of Chemical and Petroleum Engineering, 59(2), 197-207. 10.22059/jchpe.2025.387006.1582.

[14] Tanhaei, H., & Dehaghani, A. H. S. (2025). Independent effects of microwave irradiation and acidic solutions on asphaltene content and upgrading of heavy crude oil. *Journal of Molecular Liquids*, *431*, 127743. https://doi.org/10.1016/j.molliq.2025.127743.

[15] Tanhaei, H., & Saeedi Dehaghani, A. H. (2025). Improvement of the quality of heavy crude oil and reducing the concentration of asphaltene hydrocarbons using microwave radiation during acidizing. Scientific Reports, 15(1), 7434. https://doi.org/10.1038/s41598-025-91932-x.

[16] Behnammotlagh, M. A., Hashemi, R., Taheri Rizi, Z., Mohammadtaheri, M., & Mohammadi, M. (2022). Experimental study of the effect of the combined monoethylene glycol with NaCl/CaCl2 salts on sour gas hydrate inhibition with low-concentration hydrogen sulfide. Journal of Chemical & Engineering Data, 67(5), 1250-1258. https://doi.org/10.1021/acs.jced.1c00888.

[17] Fredd, C. N., & Fogler, H. S. (1998). Influence of transport and reaction on wormhole formation in porous media. AIChE journal, 44(9), 1933-1949. https://doi.org/10.1002/aic.69044090.

[18] Ghommem, M., Zhao, W., Dyer, S., Qiu, X., & Brady, D. (2015). Carbonate acidizing: Modeling, analysis, and characterization of wormhole formation and propagation. Journal of Petroleum Science and Engineering, 131, 18-33. https://doi.org/10.1016/j.petrol.2015.05.016 .

[19] Liu, Q., Yin, T., & Lu, Y. (2019). Modeling of wormhole propagation and dissolution in carbonate acidizing. Fuel, 238, 1–10. https://doi.org/10.1016/j.fuel.2018.10.133 .

[20] Useche-Narvaez, C., Montes-Páez, E. G., & Guerrero-Martin, C. A. (2022). Evaluation of the carbon footprint produced by conventional artificial lift systems in a Colombian field. Journal of Petroleum Science and Engineering, 208, 108865. https://doi.org/10.1016/j.petrol.2021.108865 .

[21] Nasr-El-Din, H. A., & Al-Humaidan, A. (2018). Recent developments in carbonate acidizing: New fluids and additives. SPE Production & Operations, 33(4), 768–784. https://doi.org/10.2118/194139-PA .

[22] Meng, Z., Li, Y., Yang, Y., Xu, Z. Q., Shi, B., & Zhao, S. L. (2015). Effect of a nanoparticulate anti-friction coating on galling resistance of threaded oil-casing couplings. Journal of Petroleum Science and Engineering, 128, 140-144. https://doi.org/10.1016/j.petrol.2015.02.008 .

[23] Nande, S. B., Al-Shalabi, E. W., & Rao, D. N. (2021). A review of low-salinity and smart-waterflooding mechanisms in carbonates. Energy Reports, 7, 507–519. https://doi.org/10.1016/j.egyr.2021.01.047 .

[24] Buriro, M. A., Al-Yaseri, A., Zhang, Y., & Iglauer, S. (2024). Statistical analysis of ionic interactions for engineered-water design in carbonates. Journal of Petroleum Science and Engineering, 235, 112756. https://doi.org/10.1016/j.petrol.2024.112756 .

[25] Karimi, M., Mahzari, P., Ayatollahi, S., & Hamouda, A. A. (2016). Wettability alteration and oil recovery by brine formulation and surfactant in carbonates. Journal of Petroleum Science and Engineering, 146, 416–428. https://doi.org/10.1016/j.petrol.2016.06.005 .

[26] Noorizadeh Bajgirani SS, Saeedi Dehaghani AH. Experimental investigation of wettability alteration, IFT reduction, and injection schemes during surfactant/smart water flooding for EOR application. Sci Rep. 2023 Jul 13;13(1):11362. doi: 10.1038/s41598-023-37657-1.

[27] Chukwuma, M., Mahmoud, M. A., Al-Khaldi, M. H., & Aljawad, M. S. (2022). Hybrid acid systems for carbonate stimulation: Experimental insights and modeling perspectives. Fuel, 316, 123356. https://doi.org/10.1016/j.fuel.2022.123356 .

[28] Parandeh, F., Zolfaghari, A., & Sadeghi, M. (2023). Acidizing performance of blended HCl–organic systems under high-temperature carbonate conditions. Petroleum Science and Technology, 41(14), 1721–1733. https://doi.org/10.1080/10916466.2023.2194718 .

[29] Meisam Mohammadzadeh Shirazi, Shahab Ayatollahi, Cyrus Ghotbi .(2019). Damage evaluation of acid-oil emulsion and asphaltic sludge formation caused by acidizing of asphaltenic oil reservoir,Journal of Petroleum Science and Engineering, Volume 174,2019,Pages 880-890,ISSN 0920-4105, https://doi.org/10.1016/j.petrol.2018.11.051.

[30] Kalhori, P., Mahmoud, M. A., & Al-Yaseri, A. (2025). A comprehensive review on acid-induced sludge: Mechanisms and controlling factors. Chemical Engineering Journal, 491, 142368. https://doi.org/10.1016/j.cej.2024.142368 .

[31] Jafari, R., & Madadizadeh, M. (2025). CTAB-assisted acidizing and wettability modification for improved carbonate recovery. Energy & Fuels, 39(7), 11290–11306. https://doi.org/10.1021/acs.energyfuels.5c02547 .